Control of Distributed Generation Systems—Part II: Load Sharing Control

Mohammad N. Marwali, *Member, IEEE*, Jin-Woo Jung, *Student Member, IEEE*, and Ali Keyhani, *Fellow, IEEE*

***Abstract*—This paper is concerned with the control strategy for the parallel operation of distributed generation systems (DGS) in a standalone ac power supply. The proposed control method uses only low-bandwidth data communication signals between each generation system in addition to the locally measurable feedback signals. This is achieved by combining two control methods: droop control method and average power control method. The average power method with slow update rate is used in order to overcome the sensitivity about voltage and current measurement errors. In addition, a harmonic droop scheme for sharing harmonic content of the load currents is proposed based on the voltages and currents control algorithm presented in [28]. Experimental and simulation studies using two parallel three-phase pulsewidth modulation (PWM) inverters are presented to show the effectiveness of the proposed control.**

***Index Terms*—Distributed generation systems (DGS), pulsewidth modulation (PWM) inverters.**

I. Introduction

RECENTLY, interest in distributed generation systems (DGS) is rapidly increasing, particularly onsite generation. This interest is due to the facts that larger power plants are economically unfeasible in many regions due to increasing system and fuel costs, and stricter environmental regulations. In addition, recent technological advances in small generators, power electronics, and energy storage devices have provided a new opportunity for distributed energy resources at the distribution level, and especially, the incentive laws to utilize renewable energies have also encouraged a more decentralized approach to power delivery [1]–[16].

There exist various generation sources for DGS: conventional technologies (diesel or natural gas engines), emerging technologies (micro turbines or fuel cells or energy storage devices) [2], [4], [6]–[12], and renewable technologies (small wind turbines or solar/photovoltaic or small hydro turbines) [3], [4], [10]. These DGS are used for applications to a standalone [11], [12], [16], a standby [2], [9], a grid-interconnected [12], a cogeneration [7]–[9], peak shavings [2], etc. and have many advantages such as environmental-friendly and modular electric generation, increased reliability, high power quality, uninterruptible service, cost savings, on-site generation, expandability, etc.

Manuscript received January 29, 2003; revised October 24, 2003. This work was supported in part by the National Science Foundation under Grant ECS ECS-0118080 and by the Ohio State University Mechatronics Laboratory. Recommended by Associate Editor B. Fahimi.

The authors are with the Department of Electrical and Computer Engineering, Ohio State University, Columbus, OH 43210 USA (e-mail: mmarwali@ameritech.net; jungj@ece.osu.edu; keyhani@ece.osu.edu).

Digital Object Identifier 10.1109/TPEL.2004.836634

Introduction of such DGS as combustion engine, small hydro, photovoltaic arrays, fuel cells, micro turbines, or battery energy storage systems, and cogenerations into power systems is very attractive for power utility companies, customers, and societies. This is true for power utility companies, since DGS can help improve power quality and power supply flexibility, maintain system stability, optimize the distribution system, provide the spinning reserve and reduce the transmission and distribution cost, and can be used to feed customers in the event of an outage in the line or in the primary substation or during scheduled interruptions. Also, for societies, the renewable energy can significantly reduce the emission from the traditional power plants. So many utility companies are trying to construct small distribution stations combined with several DGS available at the regions, instead of large power plants.

Basically, these technologies are based on notably advanced power electronics because all DGS require power converters, PWM techniques, and electronic control units [1]–[16]. That is, electrical power generated by all DGS is first converted into dc power, and then all the power fed to the dc distribution bus is again converted by dc to ac power converters into an ac power with fixed magnitude and frequency by control units using a digital processing processor (DSP). Therefore, in order to permit grid interconnection of asynchronous generation sources, advanced power electronic technologies are definitely required.

The research works in the recent papers about DGS focus on two applications: a standalone ac system and a grid-interconnection to the utility mains. In a standalone ac power supply, several DGS independently supply the loads with electrical power, like the parallel operation of the uninterruptible power supply (UPS) systems. In a grid-interconnected operation to ac mains, each DGS is interconnected in parallel to the utility, and it directly provides power to ac mains in order to cover increased power required by the loads.

This paper is concerned with the control strategy for the parallel operation of distributed generation systems (DGS) in a standalone ac power supply. In particular, the paper focuses on proper power sharing of each DGS such as the real power, reactive power, and harmonic power in a standalone ac power supply, like the parallel operation of multiple UPS systems [16]–[22]. First of all, good load-sharing should be maintained under both locally measurable voltages/currents and the wire impedance mismatches, voltage/current measurement error mismatches that significantly degrade the performance of load-sharing. Key features of the proposed control method are that it only uses locally measurable feedback signals (voltages/currents) and uses relatively low bandwidth data

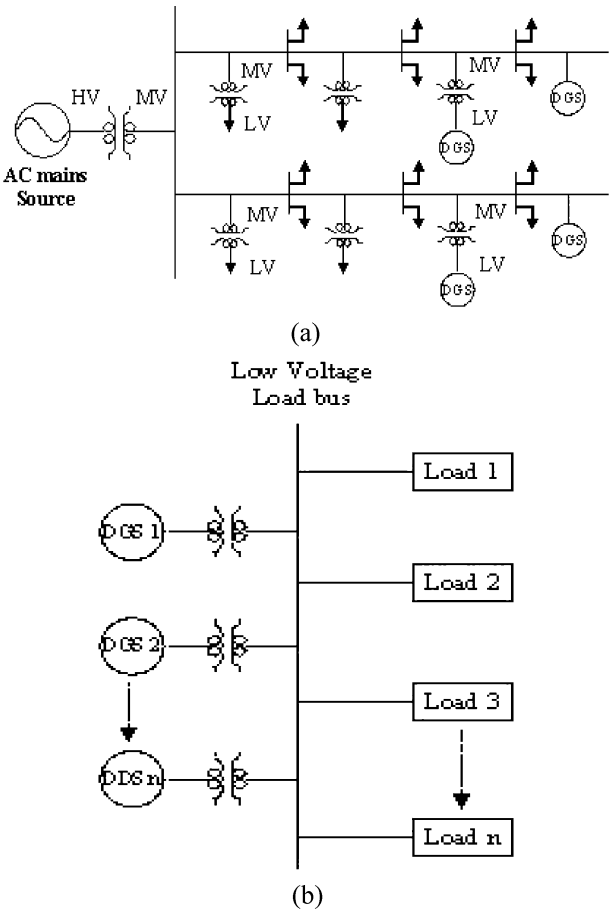

Fig. 1. Configurations for two applications of DES: (a) a grid-interconnection and (b) a standalone ac power supply.

communication signals (respective real power and reactive power) between each generation system [23]–[25].

To ensure good load-sharing, the scheme combines two control methods: droop control method and average power control method. In this method, the sharing of real and reactive powers between each DGS is implemented by two independent control variables: power angle and inverter output voltage amplitude. Especially, the average power method is used in order to significantly reduce the sensitivity about voltage and current measurement error mismatches. This scheme guarantees good load-sharing of the fundamental components of the load currents [21], [22], [26].

To ensure sharing of harmonic contents of the load currents, a harmonic droop sharing technique is proposed in this paper. The technique is based on the voltages and currents control developed in [28]. The proposed harmonic droop technique has the advantage that it only affects the harmonic compensator gains and does not degrade the fundamental voltage regulation.

In this study, two three-phase PWM inverters (600 kVA) operating in parallel are implemented by digital computer simulation using Matlab/Simulink. Some simulation results under various operating conditions are also given.

II. Distributed Energy System Description

The configurations for two applications of DGS systems are shown in Fig. 1: a grid-interconnection and a standalone ac power supply. Fig. 1(a) shows a schematic diagram of DGS used for a grid-interconnection application. As shown in Fig. 1(a), DGS are interconnected to the conventional distribution lines in order to cover increased power required by the loads, so the distributed generation systems may spread around the distributed system that is connected to a grid system. In this application, DGS are connected to Medium Voltage Network or Low Voltage Network according to power ratings or voltage ratings available for the systems. Fig. 1(b) shows the network structure of distributed generation systems used for a standalone ac power supply, and each distributed energy system supply power to the loads, like the parallel operation of UPS units in the emergency mode operation. As shown in Fig. 1(b), this architecture may require for each DGS to operate independently because the distance between DGS units may make data communication impractical and the control should be based on those variables that can only be measured locally at the inverter. However, recently data communication between units can easily be realized by the rapid advances in the field of communication.

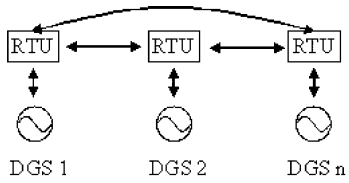

Fig. 2. Control unit communications between DGS units.

Fig. 2 shows a schematic diagram for data communication between remote terminal unit (RTU) and RTU for each DES to exchange power information (real power and reactive power) in a standalone ac power system.

DGS circuit model in a standalone ac power system is shown in Fig. 3. This model consists of two three-phase PWM inverters running in parallel supporting two loads. The power converter of each DGS studied in this paper is a dc/ac voltage source inverter, and each inverter is equipped with an LC output filter and a Δ/Y transformer (600 kVA, $N_p : N_s = 245 : 208$). In this figure, in order to simplify circuit analysis, generation sources such as combustion engine, small hydro, photovoltaic arrays, fuel cells, micro turbines or battery energy storage systems, etc., can be modeled as dc voltage sources (VDC1 and VDC2).

III. DGS Control Requirements

In general, the droop technique [16]–[22], [27] has been widely used as a load-sharing scheme in conventional power system with multiple generators. In this droop method, the generators share the system load by drooping the frequency of each generator with the real power (P) delivered by the generator. This allows each generator to share changes in total load in a manner determined by its frequency droop characteristic and essentially utilizes the system frequency as a communication link between the generator control systems [16]–[20]. Similarly, a droop in the voltage amplitude ($V_{\max}$) with reactive power (Q) is used to ensure reactive power sharing.

This load sharing technique is based on the power flow theory in an ac system, which states that the flow of the active power

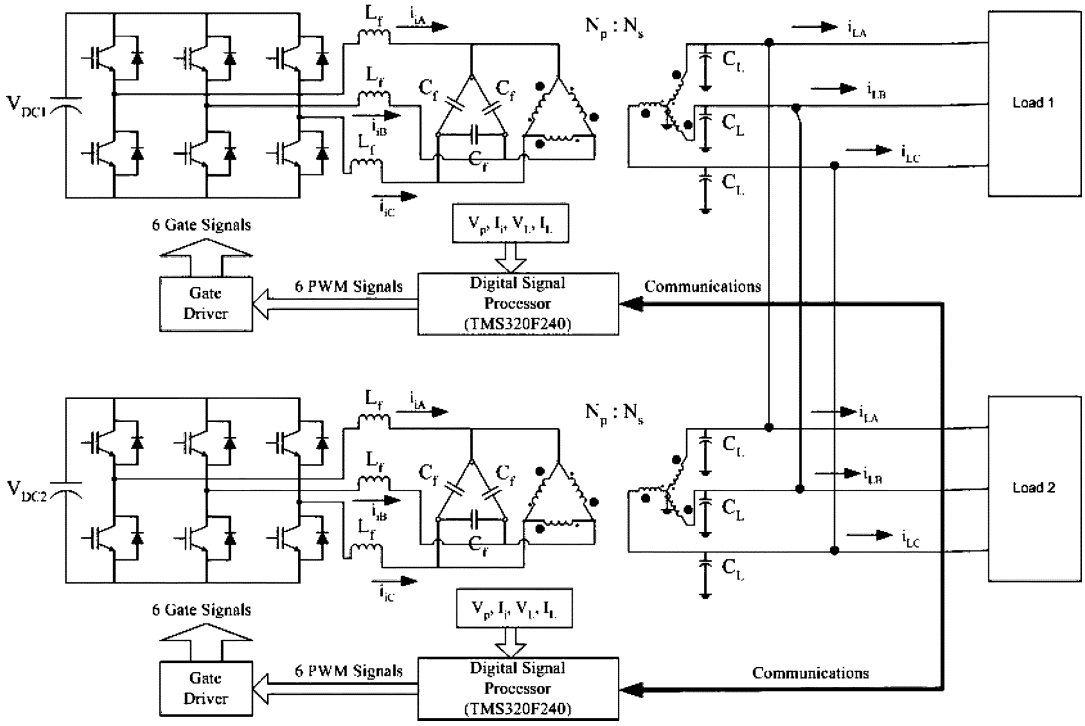

Fig. 3. DGS circuit model in a standalone ac power system.

(P) and reactive power (Q) between two sources can be controlled by adjusting the power angle and the voltage magnitude of each system—i.e., the active power flow (P) is predominantly controlled by the power angle, while the reactive power (Q) is predominantly controlled by the voltages magnitude. This theory is explained in Fig. 4. Fig. 4 indicates critical variables for load-sharing control of paralleled power converters. Fig. 4 shows two inverters represented by two voltage sources connected to a load through line impedance represented by pure inductances L_1 and L_2 for simplified analysis purpose.

The complex power at the load due to inverter i is given by

$$S_i = P_i + jQ_i = V \cdot I_i^* \tag{1}$$

where $i = 1, 2$, and I_i^* is the complex conjugate of the inverter i current and is given by

$$I_i^* = \left[\frac{E_i \cos\delta_i + jE_i \sin\delta_i - V}{j\omega L_i}\right]^* \tag{2}$$

$$\therefore\ S_i = V\left[\frac{E_i \cos\delta_i + jE_i \sin\delta_i - V}{j\omega L_i}\right]^*. \tag{3}$$

This gives the active and reactive power flowing from the ith inverter as

$$P_i = \frac{VE_i}{\omega L_i}\sin\delta_i \tag{4}$$

$$Q_i = \frac{VE_i \cos\delta_i - V^2}{\omega L_i}. \tag{5}$$

From (1)–(5), it can be seen that, if δ_1 and δ_2 are small enough, then the real power flow is mostly influenced by the power angles δ_1 and δ_2, while the reactive power flow predominantly depends on the inverter output voltages E_1 and E_2. This means that to certain extent the real and reactive power flow can be controlled independently. Since controlling the frequencies dynamically controls the power angles, the real power flow control can be equivalently achieved by controlling the frequencies of the voltages generated by the inverters.

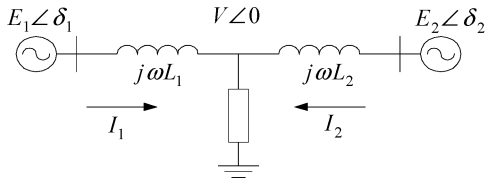

Fig. 4. Two inverters connected to a load.

Therefore, as mentioned above, the power angle and the inverter output voltage magnitude are critical variables that can directly control the real and reactive power flow for proper load-sharing of power converters connected in parallel.

Similarly, the above control theory can be applied to parallel operation of distributed energy systems in a standalone ac power supply application. In general, there is large distance between inverter output and load bus, so each DGS is required to operate independently as using only locally measurable voltages/currents information. In addition, there is also long distance between DGS units, so data communication between DGS units may be impractical [16]–[20]. However, in recent years, data communication between DGS units can easily be implemented by the rapid advances in the field of communication.

Therefore, the paper considers the parallel operation of power converters in a standalone ac system under signal communications between units in order to ensure exact load-sharing

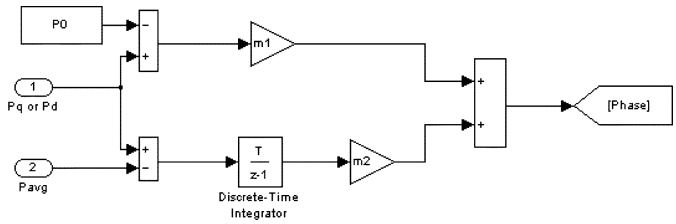

Fig. 5. Real power ($P_{\rm q}$ or $P_{\rm d}$) sharing control.

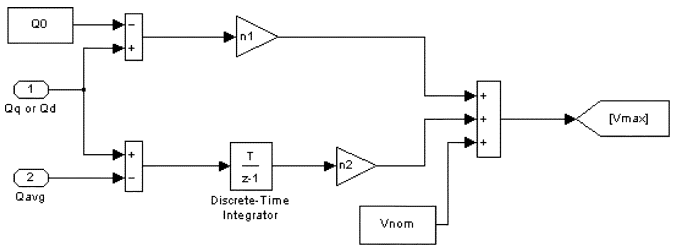

Fig. 6. Reactive power ($\rm Q_q$ or $\rm Q_d$) sharing control.

of each DGS unit. In particular, this research focuses on proper load-sharing between each unit, and the load-sharing should be also guaranteed under the wire impedance mismatches, voltage/current measurement error mismatches, and interconnection tie-line impedance effect that can heavily affect the performance of load-sharing [20]–[22].

Control constraints considered in this paper are summarized as follows:

1) locally measurable feedback signals (voltages/currents);
2) data communications between each DGS about real power and reactive power;
3) wire impedance mismatches between inverter output and load bus;
4) voltage/current sensor measurement error mismatches;
5) tie-line impedance between loads.

To overcome the above control constraints, a new droop technique using both average power method and harmonic droop control is proposed.

IV. Proposed Load Sharing Control Algorithm

A. Combined Droop Control Method and Average Power Control Method

In order to guarantee exact load-sharing of the real power (P) and the reactive power (Q) between DGS units, the conventional droop method should be modified by a new control algorithm. To do this, a combination of the droop method, the average power control method, and harmonic sharing control loop is proposed for load-sharing of paralleled inverters. Fig. 5 shows a Simulink block diagram for the real power sharing control. In this figure, phase angle ($\Delta\theta$ phase) is chosen as the control variable instead of frequency used as a control variable in a conventional droop method. This has the advantage that since the phase angle is not varied due to constant real power in steady-state time, the frequency remains at nominal value (60 Hz). This is in contrast to the conventional droop method that uses frequency as a control variable which may result in deviation from nominal frequency at steady-state. As shown in Fig. 5, the difference between real-time active power (P_q or P_d) of each unit and the rating real power (P_{0_qd}) of each unit is multiplied by a droop coefficient (m_1). In addition, the difference between the active power (P_q or P_d) of each DGS unit and the average real power (P_{avg_qd}) is finally equal to zero by a discrete-time integrator in steady-state time. As a result, the active power between the DGS units is properly shared according to the power ratings of each DGS unit.

The Simulink block diagram for the reactive power (Q_q or Q_d) sharing control is implemented in Fig. 6. As shown in Fig. 6,

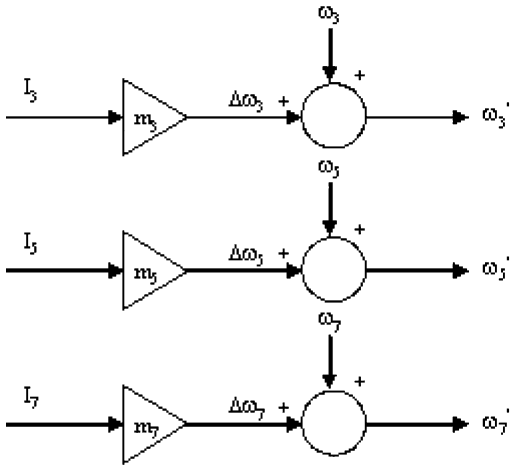

Fig. 7. Harmonic sharing droop control loop: $m_3 < 0, m_5 < 0, m_7 < 0$.

the amplitude of a reference voltage ($V_{max_q d}$) is decided by the average reactive power ($Q_{avg_q d}$) and the reactive power of each unit. The difference between real-time reactive power (Q_q or Q_d) of each unit and the rating reactive power ($Q_{0_q d}$) of each unit is multiplied by a droop gain (n1). In addition, by a discrete-time integrator, the reactive power (Q_q or Q_d) of each DGS unit is also finally equal to an average reactive power ($Q_{avg_q d}$) in steady-state time. In order that the amplitude of the reference load voltage is generated, the nominal load voltage $[\mathrm{Vnom}(480\cdot\sqrt{2})]$ is also added to the results by the droop gains of the average reactive power ($Q_{avg_q d}$) and the reactive power ($Q_{\rm q}$ or $Q_{\rm d}$).

From Figs. 5 and 6 above, the phase angle and voltage amplitude of the reference load voltage are obtained from the following equations.

Q-Axis

Phase angle

$$\begin{aligned}\phi_q(k+1) &= \phi_q(k) + m_2(P_q - P_{\rm avg\_q})\\ \Delta\theta_q(k) &= \phi_q(k) + m_1(P_q - P_{0\_q})\\ \theta_q(k) &= \theta_{\rm ref}(k) + \Delta\theta_q(k).\end{aligned} \tag{6}$$

Amplitude

$$\begin{aligned}V_q(k+1) &= V_q(k) + n_2(Q_q - Q_{\rm avg})\\ \Delta V_q(k) &= V_q(k) + n_1(Q_q - Q_{0\_q})\\ V_{\rm max\_q}(k) &= V_{\rm nom} + \Delta V_q(k).\end{aligned} \tag{7}$$

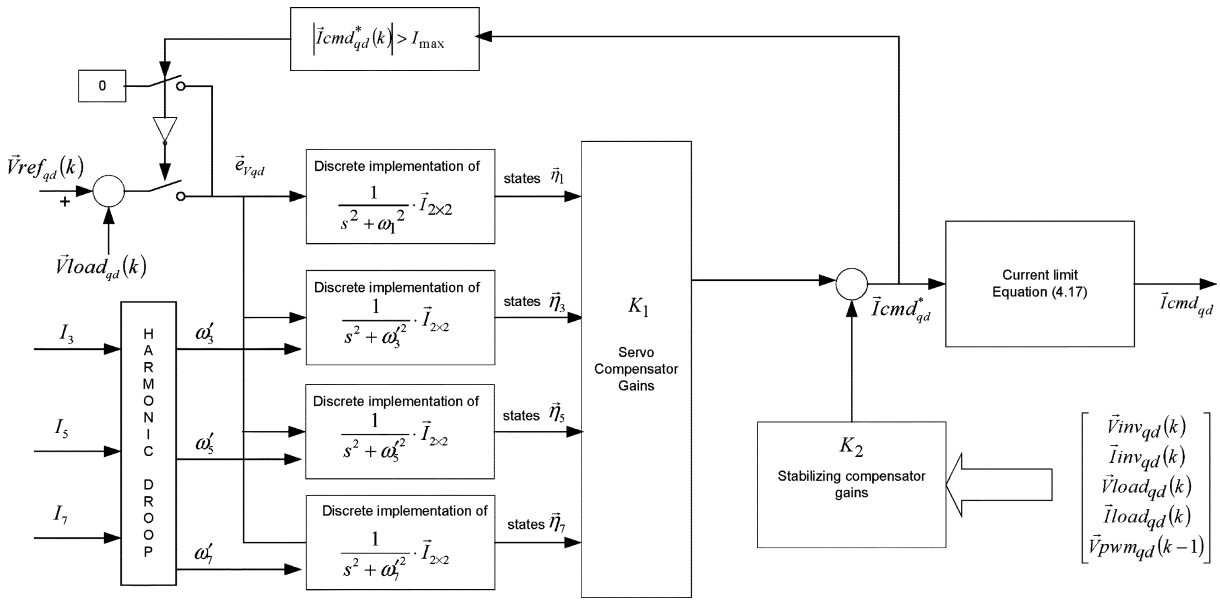

Fig. 8. Output voltages controller using robust servomechanism controller [28] with harmonic drooping.

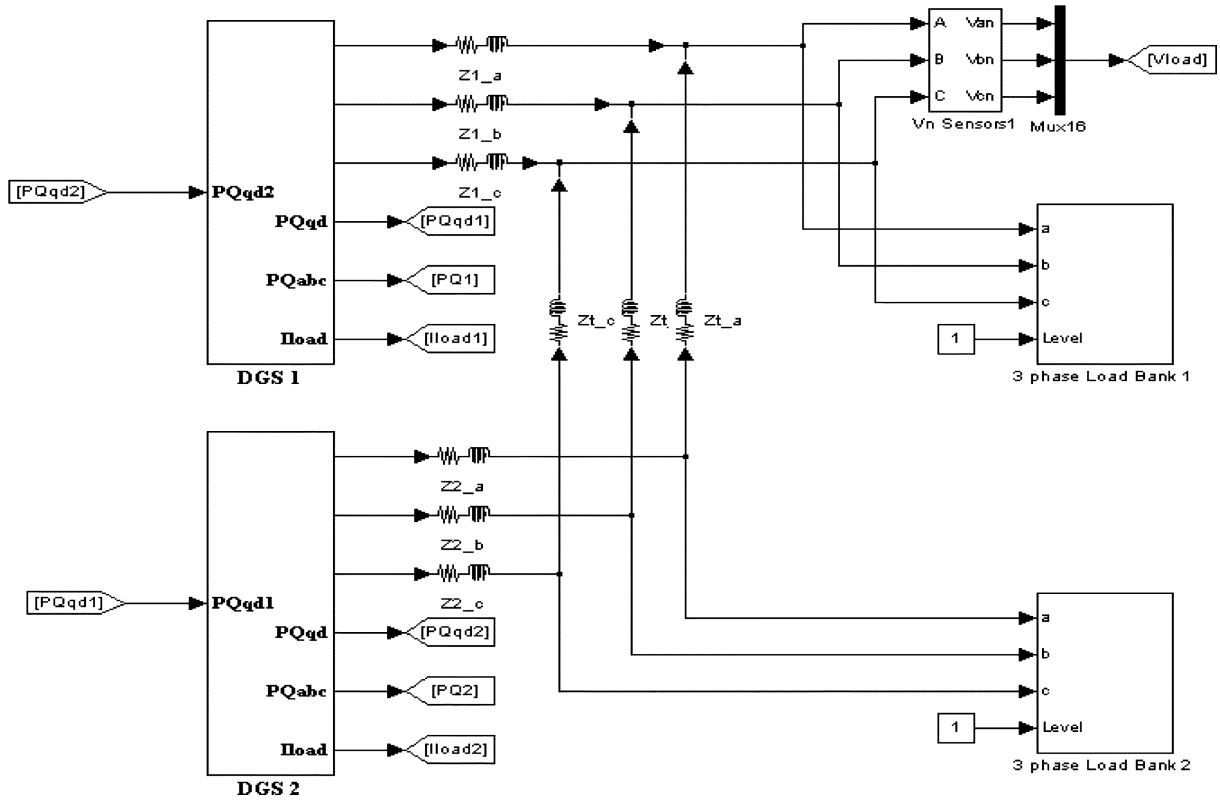

Fig. 9. Simulink model of two DGS units connected to two loads.

Voltage Reference

$$V_{\text{ref\_q}}(k) = V_{\max\_q}\cdot\sin\left(\theta_q(k)\right). \tag{8}$$

D-Axis

Phase angle

$$\begin{aligned}\phi_d(k+1) &= \phi_d(k) + m_2(P_d - P_{\text{avg\_d}})\\ \Delta\theta_d(k) &= \phi_d(k) + m_1(P_d - P_{0\_d})\\ \theta_d(k) &= \theta_{\text{ref}}(k) + \Delta\theta_d(k).\end{aligned} \tag{9}$$

Amplitude

$$\begin{aligned}V_d(k+1) &= V_d(k) + n_2(Q_d - Q_{\text{avg\_d}})\\ \Delta V_d(k) &= V_d(k) + n_1(Q_d - Q_{0\_d})\\ V_{\max\_d}(k) &= V_{\text{nom}} + \Delta V_d(k).\end{aligned} \tag{10}$$

Voltage Reference

$$V_{\text{ref\_d}}(k) = V_{\max\_d}\cdot\sin\left(\theta_d(k)\right). \tag{11}$$

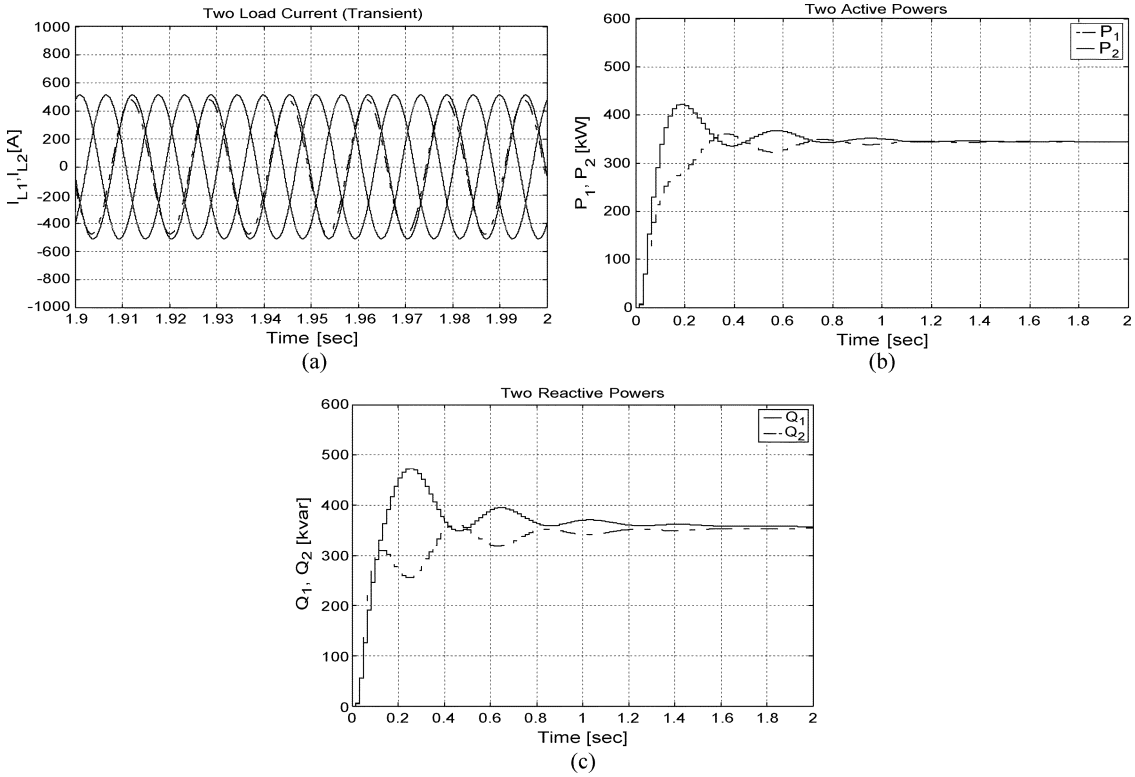

Fig. 10. Case 1 Simulation results: (a) load currents (I_{L1} and I_{L2}), (b) real powers (P_1 and P_2), and (c) reactive powers (Q_1 and Q_2).

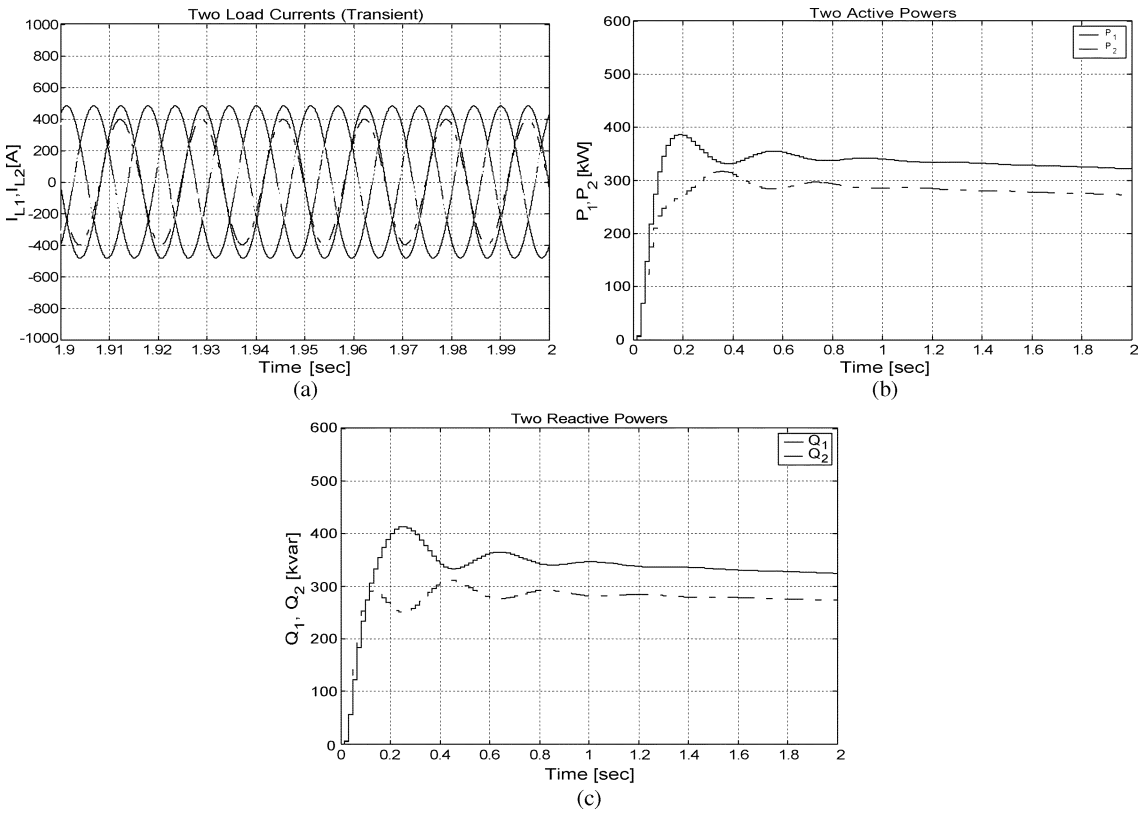

Fig. 11. Case 2 Simulation results: (a) load currents (I_{L1} and I_{L2}), (b) real powers (P_1 and P_2), and (c) reactive powers (Q_1 and Q_2).

m_1 and n_1 are the droop gain for real power and reactive power, respectively; m_2, n_2 error gain between average real power ($P_{\mathrm{avg\_}qd}$), and real power (P_{qd}) of each unit, average reactive power ($Q_{\mathrm{avg\_}qd}$) and reactive power (Q_{qd}) of each unit, respectively; P_{0_qd}, Q_{0_qd} are real and reactive power rating of each unit, respectively; V_{nom}, f_{nom} are nominal voltage amplitude ($480 \cdot \sqrt{2}\ V$), nominal frequency (60 Hz), respectively, $\theta_{\mathrm{ref}} : 2 \cdot \pi \cdot f_{\mathrm{nom}} \cdot t$.

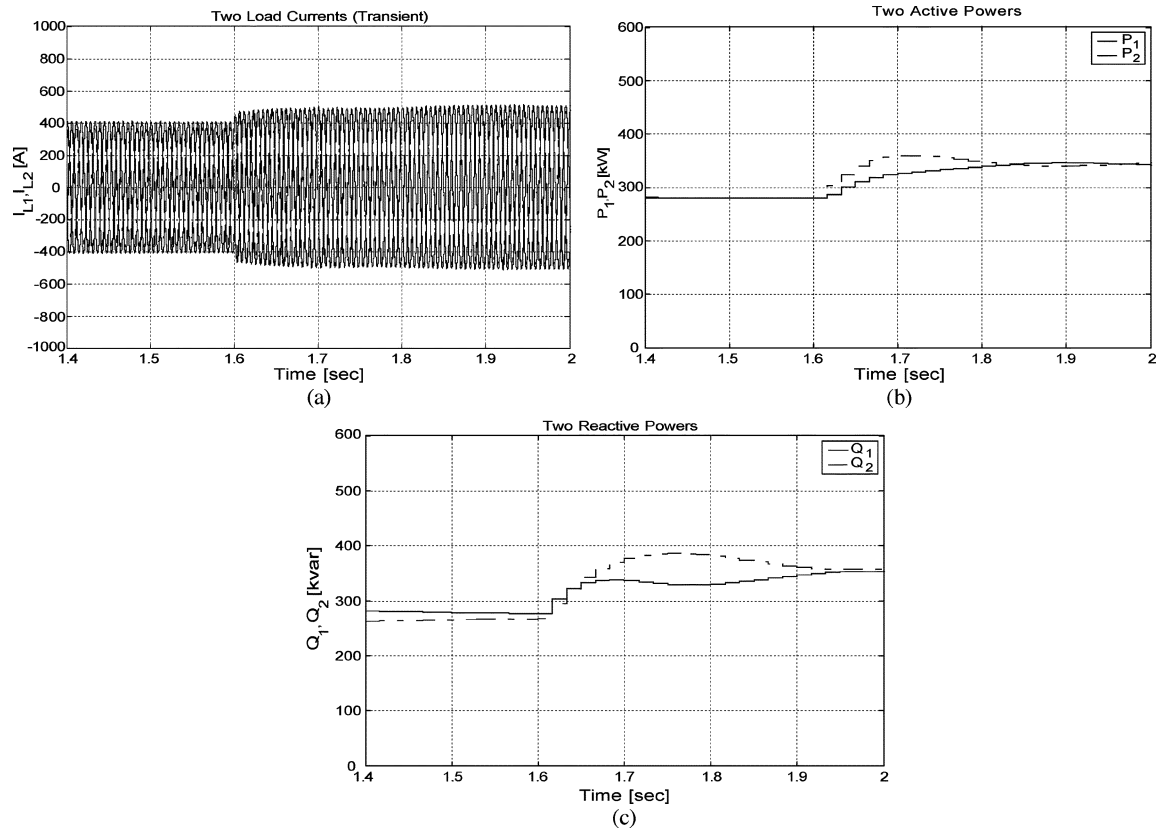

Fig. 12. Case 3 Simulation results: (a) load currents ($I_{\mathrm{L}1}$ and $I_{\mathrm{L}2}$) (b) real powers (P_1 and P_2), and (c) reactive powers (Q_1 and Q_2).

B. Harmonic Sharing Control Loop

The above combined droop method and average power control method does not guarantee the harmonic components of the load current to share because it affects only the phase and magnitude of the fundamental output voltage. A means is required to share the harmonic components of the load currents based on its harmonic contents. The control gains affecting the harmonics in the voltage controller designed in [28] can be adjusted based on the harmonic contents of the load current at that harmonic frequency. For example, the pole frequencies of the harmonic compensator can be shifted by the harmonic contents of the load current at those frequencies. This is illustrated in Fig. 7, where I_3, I_5, and I_7 denote the harmonic load currents at third, fifth, and seventh harmonics respectively, and ω_3', ω_5', and ω_7' are the third, fifth, and seventh harmonic frequencies of the harmonic compensator poles. First of all, the harmonic droop loop added has the advantage that it does not degrade the fundamental component; it only affects the individual harmonic when it exists.

The ω_3', ω_5', and ω_7' are computed from the harmonic droop control in Fig. 7

$$\begin{aligned}\omega_3' &= \omega_{3+} m_3 I_3, \quad \omega_3 = 2\pi \cdot 3 \cdot 60 \\ \omega_5' &= \omega_{5+} m_5 I_5, \quad \omega_5 = 2\pi \cdot 5 \cdot 60 \\ \omega_7' &= \omega_{7+} m_7 I_7, \quad \omega_7 = 2\pi \cdot 7 \cdot 60.\end{aligned}$$

The resulting voltage controller developed in [28] with the harmonic drooping control added is shown in Fig. 8.

V. Simulation Results

Simulations were performed using Matlab/Simulink v6.1 with power system block-set (PSB). For speed of simulations, the PWM bridge IGBT inverter has been modeled as an ideal voltage controlled source with a delay of half the sampling time of the actual PWM signal. Fig. 9 shows Simulink block diagrams for the simulated distributed generation systems. This model is composed of two DGS units, two loads, wire impedances (Z_1 and Z_2), and tie-line impedance. Two linear transformers are used for the isolation transformers, and a series inductance and resistance representing the leakage impedance and losses of each transformer are respectively 3% p.u. The series inductance and resistance of the transformers are denoted as L_T and R_T, respectively. The powers information is exchanged between units every 0.5 s.

The nominal values of the circuit components for simulations are as follows:

$$\begin{aligned}&\text{Rated Output Power of Each DGS System} = 600 \text{ kVA} \\ &\text{ac Load Voltage} = 480 \text{ V (rms)} \\ &\frac{\Delta}{Y}\text{transformer} = 600 \text{ kVA}, \quad \frac{980 \text{ V}}{480 \text{ V}}, \quad 60 \text{ Hz} \\ &V_{\mathrm{dc}} = 2200 \text{ V ac}, \quad \text{PWM Frequency} = 5.4 \text{ kHz} \\ &T_s(\text{sampling period}) = 185\ \mu\text{s} \\ &T_d(\text{delay time}) = \frac{T_s}{2} \\ &L_f = 5 \text{ mH}, \quad C_f = 300\ \mu\text{F} \\ &L_T = 31\ \mu\text{H} \quad R_T = 0.0115\ \Omega, \quad C_L = 90\ \mu\text{F}.\end{aligned}$$

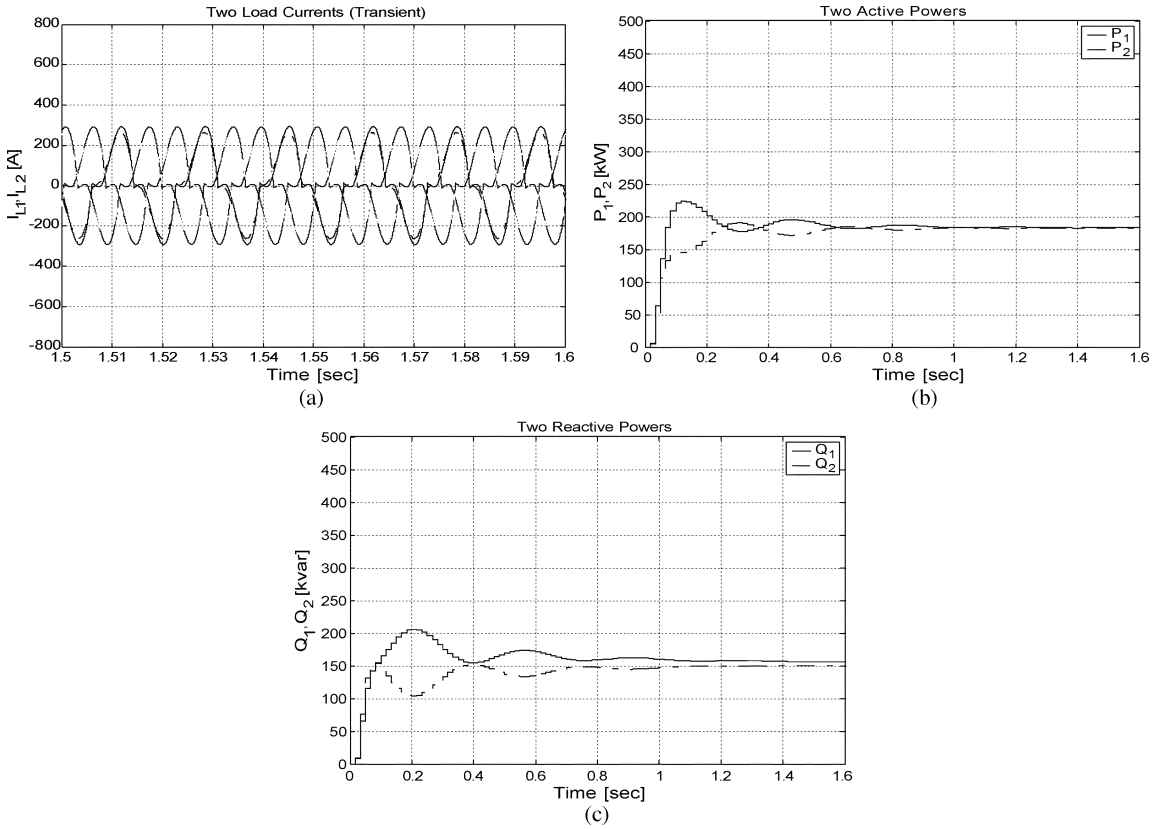

Fig. 13. Case 4 Simulation results: (a) load currents ($I_{\mathrm{L}1}$ and I_{L_2}), (b) real powers (P_1 and P_2), and (c) reactive powers (Q_1 and Q_2).

As explained in previous section, each PWM inverter's output voltage and current are controlled using dual loop control system, with outer loop (RSC) controlling the output voltage and the inner loop (DSMC) controlling the inverter current.

The droop coefficients are given as

$$m_1 = -2e-6 \text{ rad/W} \quad m_2 = -10e-6 \text{ rad/W}$$
$$n_1 = -2e-4 \text{ V/var} \quad n_2 = -20e-4 \text{ V/var} \quad .$$
$$m_3 = m_5 = m_7 = -2e-2$$

In this study, the two PWM inverters are assumed to have identical characteristics, i.e., they have matched circuit components equal to their nominal values. To verify the performance of the proposed droop method for load-sharing control, tie-line impedance, wire impedances mismatches and voltage/current sensor measurement error mismatches are considered in this simulation.

The following cases are simulated.

All Cases

Unit 1: $Z_1 = R_1 + jX_1 (R_1 = 0.01\,\Omega / L_1 = 0.5\,\text{mH})$.

Voltage measurement error:

$V_{\mathrm{P}}[-0.1\%, +0.1\%, -0.1\%]$

$V_{\mathrm{L}}[+0.1\%, +0.1\%, -0.1\%]$.

Current measurement error:

$I_{\mathrm{i}}[+0.1\%, -0.1\%, -0.1\%]$

$I_{\mathrm{L}}[+0.1\%, -0.1\%, -0.1\%]$.

Unit 2: $Z_2 = R_2 + jX_2 (R_2 = 0.02\,\Omega / L_2 = 1\,\text{mH})$.

Voltage measurement error:

$V_{\mathrm{P}}[+0.1\%, -0.1\%, +0.1\%]$

$V_{\mathrm{L}}[-0.1\%, -0.1\%, +0.1\%]$.

TABLE I
SYSTEM PARAMETERS

DC Bus Voltages	
Vdc	*540 V* (nom.) 390V (min)
AC Output voltage	
Vload	208V(LL-RMS), 120V(LN)
f	60 *Hz*
Inverter filters	
C_{inv}	540 μF
L_{inv}	300 μH
Delta-Wye Transformer	
	245V:208V, 60Hz
L_{trans}	48 μH ($\approx$ 0.03 p.u)
R_{trans}	0.02 ohm
Output filter	
C_{grass}	90 μF

Current measurement error:

$I_{\mathrm{i}}[-0.1\%, +0.1\%, +0.1\%]$ $I_{\mathrm{L}}[-0.1\%, +0.1\%, +0.1\%]$

$Z_{\mathrm{t}} = R_{\mathrm{t}} + jX_{\mathrm{t}} (R_{\mathrm{t}} = 0.02\,\Omega / L_{\mathrm{t}} = 1\,\text{mH})$.

Case 1

Power ratings of DGS unit 1 and 2: 600 k VA, respectively.

Load 1: $P_{\mathrm{load1}} = 480\,\text{kW} / Q_{\mathrm{load1}} = 360\,\text{kVar}$ (p.f. = 0.8).

Load 2: $P_{\mathrm{load2}} = 480\,\text{kW} / Q_{\mathrm{load2}} = 360\,\text{kVar}$ (p.f. = 0.8).

Case 2:

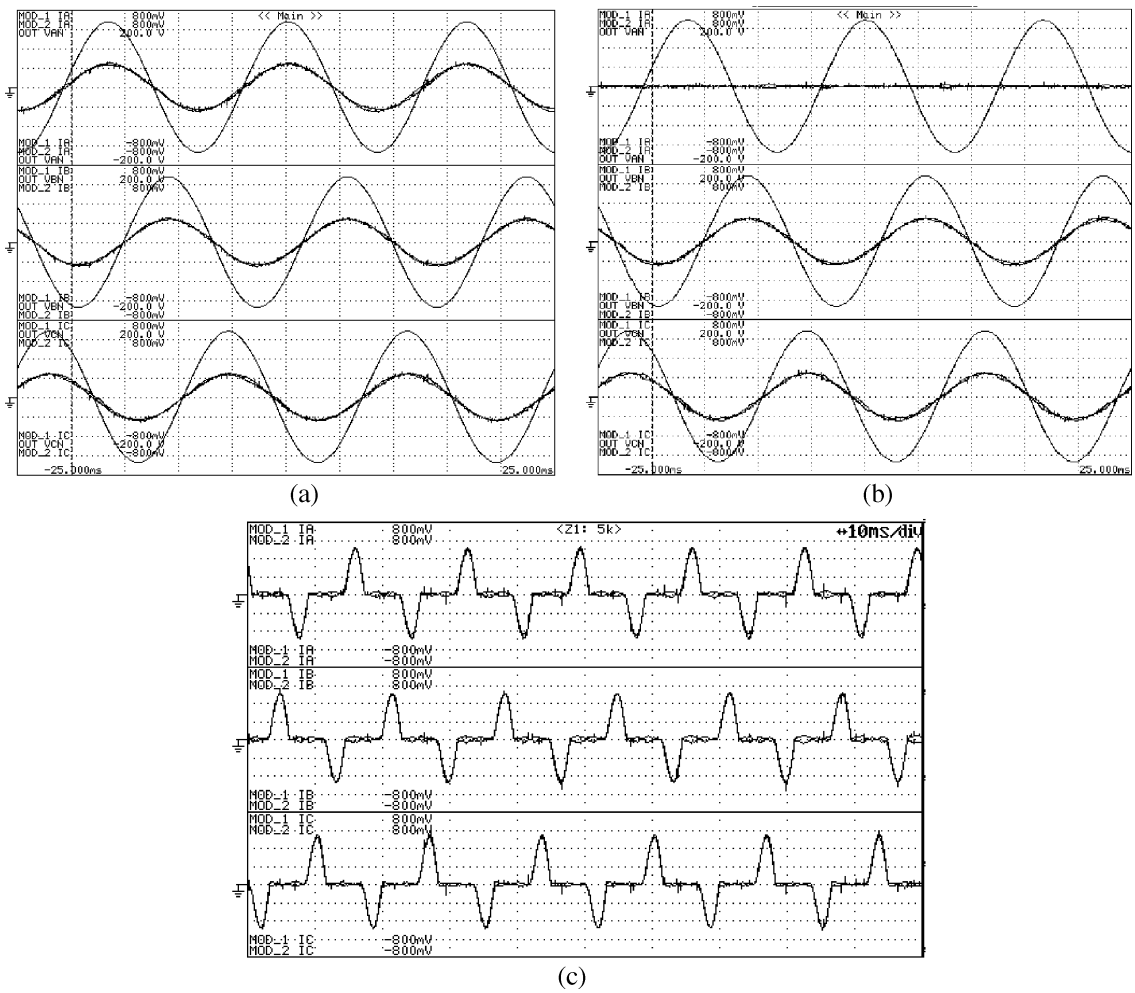

Fig. 14. Steady-state load sharing performance (a) balanced resistive load (b) unbalanced resistive load (c) balanced nonlinear rectifier load. For (a) and (b), each trace box shows the per-phase load voltage and the two units' output currents. For (c) only the two units' output currents are shown. From top to bottom the quantities apply for phase a, b, and c, respectively.

Power ratings of DGS unit 1 and 2: 600 kVA, 500 kVA, respectively.

Load 1: $P_{\text{load1}} = 400$ kW/$Q_{\text{load1}} = 300$ kVar (p.f. $= 0.8$).

Load 2: $P_{\text{load2}} = 480$ kW/$Q_{\text{load2}} = 360$ kVar (p.f. $= 0.8$).

Case 3:

Power ratings of DGS unit 1 and 2: 600 kVA, respectively.

Load 1: $P_{\text{load1}} = 480$ kW/$Q_{\text{load1}} = 360$ kVar (p.f. $= 0.8$).

Load 2: $P_{\text{load2}} = 240$ kW $=>$ 480 kW (after 1.6 s).

$Q_{\text{load2}} = 180$ kVar $=>$ 360 kVar.

In all cases, the interconnection impedances Z_2 is twice that of Z_1, and the signs of voltage/current sensor errors of unit 1 are opposite to those of unit 2. In Case 1, power rating and load of unit 1 are equal to those of unit 2, while in Case 2, the power ratings and loads of the two DGS units are different. In Case 3, the load on unit 2 changes at $\mathrm{t} = 1.6$ s. Finally, Case 4 is simulated under nonlinear loads with three single-phase diode rectifiers. In these simulations, the first three cases (Figs. 10–12) were done for linear loads, while the last case was simulated under nonlinear loads. Fig. 10 shows very good load-sharing of the real and the reactive powers under the conditions that both units and loads are identical. Fig. 11 shows the results under different power ratings and loads, and these results also show that the loads are properly shared according to the power capability of each unit. As shown in Fig. 12, even when the load 2 is increased suddenly to twice its value at $\mathrm{t} = 1.6$ s, good power sharing can still be achieved between the two units. Finally, the effectiveness of the load sharing algorithm under nonlinear load is verified with the results shown in Fig. 13.

VI. Experimental Results

To further verify its effectiveness, the proposed control strategy has been implemented on two experimental 80-kVA DGS units with setup as shown in Fig. 3. Each unit has identical system parameters given in Table I. The voltages and currents controllers proposed in [28] are used for each DGS units. The PWM timing is calculated through a standard space vector PWM [29] with switching frequency of 3.2 kHz.

Fig. 14(a)–(c) shows the steady-state performance of the load sharing control under various loads conditions. In Fig. 14(a), balanced three-phase resistive load is applied, while in Fig. 14(b) resistive loads are applied with unbalanced loading (phase a being unloaded). Fig. 14(c) shows the load

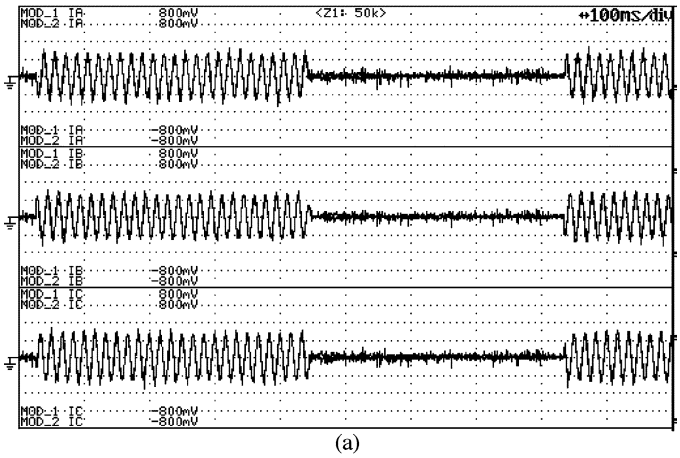

(a)

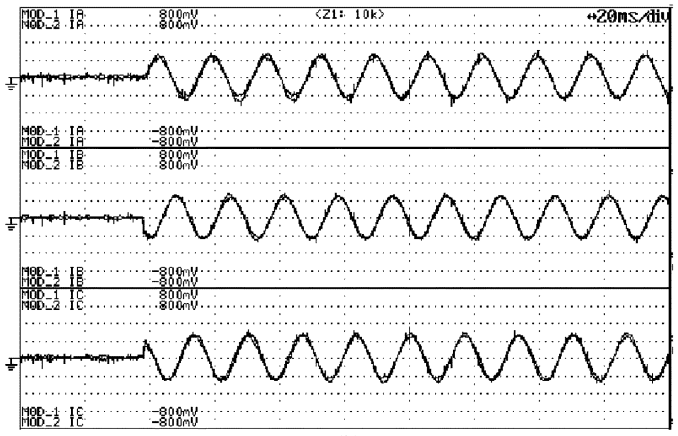

(b)

Fig. 15. Dynamic performance (a) 100% to 0% and 0% to 100% load changes and (b) 0% to 100% load acquire (zoom in). Each trace box shows the two units output currents for phase a, b, and c (from top to bottom).

sharing performance under nonlinear load in the forms of three single-phase diode rectifiers with RC loads. It can be seen that the load currents are well shared between the two units, which verifies the effectiveness of the harmonic sharing droop control.

Fig. 15 shows the performance of the load sharing control under changing load conditions. In Fig. 15(a), a 100% to 0% load change and 0% to 100% load change are shown on the same plot. Fig. 15(b) shows more detailed view of the 0 to 100% load change. It can be seen the load sharing was well maintained under both load transients.

Finally, in Fig. 16 unit 2 is brought on-line while unit 1 was supplying different types of loads on each of its phases. Phase a and b were loaded with resistive loads while phase c was loaded with a single-phase diode rectifier load. It can be seen that within a few cycles the different loads are shared by the two DGS units, verifying the effectiveness of the control under reconnection transients and its robustness toward different per-phase loading conditions.

VII. Conclusion

This paper has described a new load sharing method that can properly control the load-sharing such as the real, reactive, and harmonic powers for parallel operation of distributed generation systems in a standalone ac power system [16]–[22]. The proposed scheme is implemented by combined droop method,

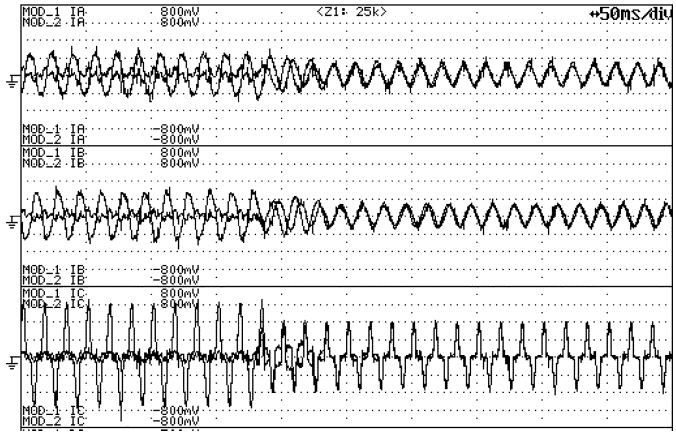

Fig. 16. Unit 2 is reconnected with different load applied on each phase. Phase a and b: linear resistive load. Phase c: single-phase nonlinear load.

average power control method, and harmonic sharing control loop using low bandwidth power information exchange between each DGS unit. In particular, the average power control method can significantly reduce the sensitivity about voltage and current measurement errors, and the harmonic control loop is added to guarantee harmonic power sharing under nonlinear loads. From the simulation and experimental results presented, it was shown that the proposed control method is very effective in maintaining proper load sharing under different types of loads including linear and nonlinear loads in standalone ac power system.

References

[1] A. Bonhomme, D. Cortinas, F. Boulanger, and J. L. Fraisse, "A new voltage control system to facilitate the connection of dispersed generation to distribution networks," in *Proc. Inst. Elect. Eng.*, 2001, p. 4.8.

[2] B. Maurhoff and G. Wood, "Dispersed generation to reduce power costs and improve service reliability," in *Proc. Rural Electric Power Conf.*, 2000, pp. C5/1–C5/7.

[3] J. Gutierrez-Vera, "Use of renewable sources of energy in Mexico," *IEEE Trans. Energy Conv.*, vol. 9, pp. 442–450, Sept. 1994.

[4] J. L. Del Monaco, "The role of distributed generation in the critical electric power infrastructure," in *IEEE-Power Engineering Soc. Winter Meeting*, vol. 1, 2001, pp. 144–145.

[5] L. Philipson, "Distributed and dispersed generation: addressing the spectrum of consumer needs," in *IEEE-Power Engineering Soc. Summer Meeting*, vol. 3, 2000, pp. 1663–1665.

[6] L. J. J. Offringa and J. L. Duarte, "A 1600 kW IGBT converter with interphase transformer for high speed gas turbine power plants," in *Proc. IEEE-Industrial Applications Soc. Conf.*, vol. 4, 2000, pp. 2243–2248.

[7] J. Gutierrez-Vera, "Mini cogeneration schemes in Mexico," in *IEEE-Power Engineering Soc. Winter Meeting*, vol. 1, 2000, pp. 651–655.

[8] D. Casadei, G. Grandi, R. K. Jardan, and F. Profumo, "Control strategy of a power line conditioner for cogeneration plants," in *Proc. IEEE Power Electronics Specialist Conf.*, vol. 2, 1999, pp. 607–612.

[9] R. K. Jardan, O. Dranga, and D. Bereknyei, "Standby power supply using alternative energy through cogeneration technologies," in *Proc. 3rd Int. Conf. TELESCON Telecommunications Energy Special*, 2000, pp. 215–219.

[10] B. Lasseter, "Microgrids," in *IEEE-Power Engineering Soc. Winter Meeting*, vol. 1, 2001, pp. 146–149.

[11] M. Etezadi-Amoli and K. Choma, "Electrical performance characteristics of a new micro-turbine generator," in *IEEE-Power Engineering Soc. Winter Meeting*, vol. 2, 2001, pp. 736–740.

[12] R. K. Jardan, I. Nagy, T. Nitta, and H. Ohsaki, "Power factor correction in a turbine-generator-converter system," in *Proc. IEEE-Induatrial Applications Soc. Conf.*, vol. 2, 2000, pp. 894–900.

[13] P. Bongrain and J. L. Fraisse, "Connection of EDF's remote control system to dispersed generation units," in *Proc. Inst. Elect. Eng.*, 2001, p. 4.7.

[14] K. Tomsovic and T. Hiyama, "Intelligent control methods for system with dispersed generation," in *IEEE-Power Engineering Soc. Winter Meeting*, vol. 2, 2001, pp. 913–917.
[15] C. Marnay, F. J. Rubio, and A. S. Siddiqui, "Shape of the microgrid," in *IEEE-Power Engineering Soc. Winter Meeting*, vol. 1, 2001, pp. 150–153.
[16] M. C. Chandorkar, D. M. Divan, and R. Adapa, "Control of parallel connected inverters in standalone ac supply systems," *IEEE Trans. Ind. Applicat.*, vol. 29, pp. 136–143, Jan./Feb. 1993.
[17] M. C. Chandorkar, D. M. Divan, Y. Hu, and Y. Banerjee, "Novel architectures and control for distributed UPS systems," in *Proc. Applied Power Electronics Conf. Expo.*, vol. 2, 1994, pp. 683–689.
[18] M. C. Chandorkar, D. M. Divan, and D. M. Banerjee, "Control of distributed UPS systems," in *Proc. Power Electronics Specialists Conf.*, vol. 1, 1994, pp. 197–204.
[19] M. C. Chandorkar and D. M. Divan, "Decentralized operation of distributed UPS systems," in *Proc. Int. Conf. Power Electronics, Drives Energy Systems Industrial Growth*, vol. 1, 1996, pp. 565–571.
[20] A. Tuladhar, H. Jin, T. Unger, and K. Mauch, "Parallel operation of single phase inverters with no control interconnections," in *Proc. IEEE Allied Power Electronic Conf.*, vol. 1, 1997, pp. 94–100.
[21] ——, "Control of parallel inverters in distributed ac power systems with consideration of line impedance effect," *IEEE Trans. Ind. Applicat.*, vol. 36, pp. 131–138, Jan./Feb. 2000.
[22] Y. B. Byun, T. G. Koo, K. Y. Joe, E. S. Kim, J. I. Seo, and D. H. Kim, "Parallel operation of three-phase UPS inverters by wireless load sharing control," in *Proc. Applied Power Electronics Conf. Expo.*, vol. 1, 2001, pp. 526–532.
[23] E. J. Davison and B. Scherzinger, "Perfect control of the robust servomechanism problem," *IEEE Trans. Automatic Control*, vol. 32, pp. 689–702, Aug. 1987.
[24] V. Utkin, J. Guldner, and J. Shi, *Sliding Mode Control in Electromechanical Systems*. Philadelphia, PA: Taylor & Franci, 1999.
[25] P. D. Ziogas, "Optimum voltage and harmonic control of PM techniques for three phase static UPS systems," *IEEE Trans. Ind. Applicat.*, vol. IA-16, pp. 542–546, July/Aug. 1980.
[26] U. B. Jensen, F. Blaabjerg, and P. N. Enjeti, "Sharing of nonlinear load in parallel connected three-phase converters," in *Proc. IEEE Industrial Applications Soc. Conf.*, vol. 4, 2000, pp. 2338–2344.
[27] S. J. Chiang and J. M. Chang, "Parallel control of the UPS inverters with frequency-dependent droop scheme," in *Proc. IEEE Power Electronics Specialist Conf.*, vol. 2, 2001, pp. 957–961.
[28] M. N. Marwali and A. Keyhani, "Control of distributed generation systems: Part I: Voltages and current control," *IEEE Trans. Power Electron.*, vol. 19, pp. ???–???, Nov. 2004.
[29] H. W. Van Der Broeck and H. C. Skudelny, "Analysis and realization of a pulsewidth modulator based on voltage space vectors," *IEEE Trans. Ind. Applicat.*, vol. 24, pp. 142–150, Jan./Feb. 1988.

Mohammad N. Marwali (M'98) received the B.S.E.E. degree from The Institut Teknologi Bandung, Bandung, Indonesia, in 1993 and the M.S.E.E degree from The Ohio State University (OSU), Columbus, in 1997, where he is currently pursuing the Ph.D degree.

His research interests are in the area of control of uninterruptible power supplies, distributed generation systems, electric motor drives, and power converters.

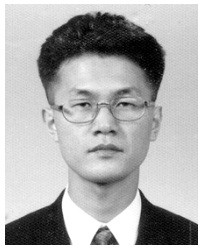

Jin-Woo Jung (S'97) received the B.S and M.S degrees in electrical engineering from Hanyang University, Korea, in 1991 and 1997, respectively, and is currently pursuing the Ph.D degree in the Department of Electrical and Computer Engineering, The Ohio State University, Columbus.

From 1997 to 2000, he was with Digital Appliance Research Laboratory, LG Electronics, Inc., Korea. His research interests are in the area of distributed generation systems, electric machines, ac motor drives, power converters, and control.

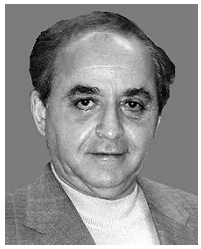

Ali Keyhani (S'72–M'76–SM'89–F'98) was with Hewlett-Packard Company and TRW Control, from 1967 to 1972. Currently, he is a Professor of electrical engineering at the Ohio State University (OSU), Columbus. He serves as the Director of OSU Electromechanical and Mechatronic Systems Laboratory. His research activities focus on the control of distributed energy systems, design and modeling of electric machine, control and design of power electronic systems, DSP-based virtual test bed for design, control of power systems, automotive systems, modeling, parameter estimation, and failure detection systems.

Dr. Keyhani received the Ohio State University College of Engineering Research Award for 1989, 1999, and 2003. He was an Editor for the IEEE TRANSACTIONS ON ENERGY CONVERSION and past Chairman of the Electric Machinery Committee, IEEE Power Engineering Society.